Comparison of online IGRT techniques for prostate IMRT treatment: Adaptive vs repositioning correction

Danthai Thongphiew, Q. Jackie Wu,[a] and W. Robert Lee
Department of Radiation Oncology, Duke University Medical Center, P.O. Box 3295, Durham, North Carolina 27710

Vira Chankong
Department of Electrical Engineering and Computer Science, Case Western Reserve University, Cleveland, Ohio 44106

Sua Yoo, Ryan McMahon, and Fang-Fang Yin
Department of Radiation Oncology, Duke University Medical Center, P.O. Box 3295, Durham, North Carolina 27710

(Received 2 October 2008; revised 4 February 2009; accepted for publication 17 February 2009; published 14 April 2009)

This study compares three online image guidance techniques (IGRT) for prostate IMRT treatment: bony-anatomy matching, soft-tissue matching, and online replanning. Six prostate IMRT patients were studied. Five daily CBCT scans from the first week were acquired for each patient to provide representative "snapshots" of anatomical variations during the course of treatment. Initial IMRT plans were designed for each patient with seven coplanar 15 MV beams on a Eclipse treatment planning system. Two plans were created, one with a PTV margin of 10 mm and another with a 5 mm PTV margin. Based on these plans, the delivered dose distributions to each CBCT anatomy was evaluated to compare bony-anatomy matching, soft-tissue matching, and online replanning. Matching based on bony anatomy was evaluated using the 10 mm PTV margin ("bone10"). Soft-tissue matching was evaluated using both the 10 mm ("soft10") and 5 mm ("soft5") PTV margins. Online reoptimization was evaluated using the 5 mm PTV margin ("adapt"). The replanning process utilized the original dose distribution as the basis and linear goal programming techniques for reoptimization. The reoptimized plans were finished in less than 2 min for all cases. Using each IGRT technique, the delivered dose distribution was evaluated on all 30 CBCT scans (6 patients $\times$5CBCT/patient). The mean minimum dose (in percentage of prescription dose) to the CTV over five treatment fractions were in the ranges of 99%–100% (SD=0.1%–0.8%), 65%–98% (SD =0.4%–19.5%), 87%–99% (SD=0.7%–23.3%), and 95%–99% (SD=0.4%–10.4%) for the adapt, bone10, soft5, and soft10 techniques, respectively. Compared to patient position correction techniques, the online reoptimization technique also showed improvement in OAR sparing when organ motion/deformations were large. For bladder, the adapt technique had the best (minimum) D90, D50, and D30 values for 24, 17, and 15 fractions out of 30 total fractions, while it also had the best D90, D50, and D30 values for the rectum for 25, 16, and 19 fractions, respectively. For cases where the adapt plans did not score the best for OAR sparing, the gains of the OAR sparing in the repositioning-based plans were accompanied by an underdosage in the target volume. To further evaluate the fast online replanning technique, a gold-standard plan ("new" plan) was generated for each CBCT anatomy on the Eclipse treatment planning system. The OAR sparing from the online replanning technique was compared to the new plan. The differences in D90, D50, and D30 of the OARs between the adapt and the new plans were less than 5% in 3 patients and were between 5% and 10% for the remaining three. In summary, all IGRT techniques could be sufficient to correct simple geometrical variations. However, when a high degree of deformation or differential organ position displacement occurs, the online reoptimization technique is feasible with less than 2 min optimization time and provides improvements in both CTV coverage and OAR sparing over the position correction techniques. For these cases, the reoptimization technique can be a highly valuable online IGRT tool to correct daily treatment uncertainties, especially when hypofractionation scheme is applied and daily correction, rather than averaging over many fractions, is required to match the original plan.
[DOI: 10.1118/1.3095767]

Key words: adaptive radiation therapy, image-guided radiation therapy, intensity-modulated radiation therapy, prostate, motion

I. INTRODUCTION

Daily setup variation and internal organ motion and deformation have long been a concern for external beam radiation therapy (EBRT) of prostate cancer. To account for these variations and to ensure adequate target coverage, margins are added around the clinical target volume (CTV) to form a planning target volume (PTV).[1,2] However, adding margins may result in a large increase in the irradiated volume,[3–5] which consequently exposes a significant amount of healthy tissue to high radiation doses.

To minimize daily treatment variations, image guided radiation therapy (IGRT) technology has been widely adopted to provide real-time geometric and anatomic information with the patient in the treatment position. In practice, online image guidance has been largely focused on shifting the patient positions by matching the daily images to the planning images, based on either bony landmarks or soft-tissue structures. Bony structure matching based correction is typically performed on a treatment system equipped with kV x-ray imaging or a megavoltage portal imaging device. For these systems, patient repositioning can be performed using 2D-2D or 2D-3D image registration. The 2D-2D correction is generally performed with orthogonal kV or MV images registered to two digital reconstructed radiograph (DRR) images projected from the planning CT volume.[6,7] The 2D-3D registration can be achieved by adjusting the position and orientation of the CT data so that the bony structures on the DRRs match the daily kV/MV images.[8–11]

Recently, patient repositioning using soft-tissue matching has also been widely implemented due to the development of cone-beam CT (CBCT), which provides volumetric information within a few minutes.[12] CBCT guided online correction is three dimensional (3D) and can be performed based on both bony and soft-tissue matching. Various 3D soft-tissue matching techniques have been proposed where the contours from planning CT images are matched with CBCT images,[13–15] or where the planning CT images and CBCT images are matched based on grayscale values.[16–19] Most of the above clinical IGRT protocols only include translational positioning corrections due to couch motion limitations. New developments in 6D couches will make rotational positioning corrections possible.[20,21]

To further take advantage of online image guidance, recent studies[13–16] have been moving toward online correction techniques based on treatment plan adaptation. Online plan adaptation not only corrects for patient positioning variations but also for changes in target volume and shapes which cannot be corrected by translations and/or rotations alone. Field aperture adjustments for 3D conformal plans have demonstrated improvement in target coverage and organ sparing.[17] Replanning techniques such as modifying fluence maps or MLC segments for IMRT plans have also been explored.[14,15,18,19,22,23] Online image guidance has also been used to perform offline modification of a patient-specific PTV.[24–27] Recently, we have proposed a novel online adaptive radiation therapy strategy for intensity-modulated plans.[28] This technique can account for large anatomical variations including both rigid and nonrigid changes. It utilizes a fast reoptimization scheme and a deformable registration tool to modify the original IMRT treatment plan, and the inverse plan solution can be achieved within 2 min.

In this study, we explored the application of this online replanning technique to prostate cancer and compared the results with the widely practiced repositioning techniques based on bony or soft-tissue matching. All patients were planned with IMRT using the standard treatment protocol at our institution. Planning margins of 5 and 10 mm were also combined with these different IGRT techniques to assess the proper margins for each technique. The target coverage and organ-at-risk (OAR) sparing of each IGRT technique was evaluated. Finally, a new plan ("new" plan) was generated based on the CBCT anatomy using the same commercial treatment planning system. The OAR sparing from the online replanning technique was compared to the new plan to evaluate the effectiveness of our new reoptimization technique.

II. MATERIALS AND METHODS

II.A. Patient data and treatment plans

Six patients receiving IMRT treatment to the prostate (including seminal vesicles) were retrospectively studied. A planning CT image set of each patient was acquired using a CT simulator (Lightspeed; GE Healthcare Technologies, Waukesha, WI) with 1 mm in-plane resolution and 3 mm slice thickness. Structures-of-interest (SOIs) were the CTV (including prostate and seminal vesicles) and OARs (including bladder and rectum). Femoral heads were also assigned as OARs during original planning but not evaluated in this study. Two PTVs were designed: (1) A PTV with conventional 10 mm expansion except in the posterior direction which was 7 mm expansion ("PTV10") and (2) a PTV with 5 mm uniform margin ("PTV5"). Here, the margin of 5 mm was studied for the possibility of margin reduction under IGRT implementation.

Two initial IMRT plans were optimized on the commercial treatment planning system (Eclipse, Varian Medical System, Palo Alto, CA), one using PTV10 and another using PTV5. Each plan used seven coplanar 15 MV beams. The primary dose constraints were adopted from the Radiation Therapy Oncology Group protocols[29] and were expected to be easily met by the IMRT plans. More stringent secondary dose constraints were set using institutional template constraints based on the target dose of 78 Gy to achieve as much sparing as possible. The dose limits to the bladder were 70, 62, and 39 Gy (to $<$20%, 30%, and 50% volumes) and the dose limits to the rectum were 70, 56, and 39 Gy (to $<$20%, 30%, and 50% volumes). A priority weight for each constraint was also assigned to gain a better control in balancing target coverage and OAR sparing. A trial-and-error scheme was used to manually adjust these constraints and the associated weights during the optimization process.[30] The total planning time for a prostate IMRT plan typically takes about 30–45 min. The planning data (the planning CT images, SOIs, beam arrangement, and the dose distribution) were exported to an in-house adaptive treatment planning platform.

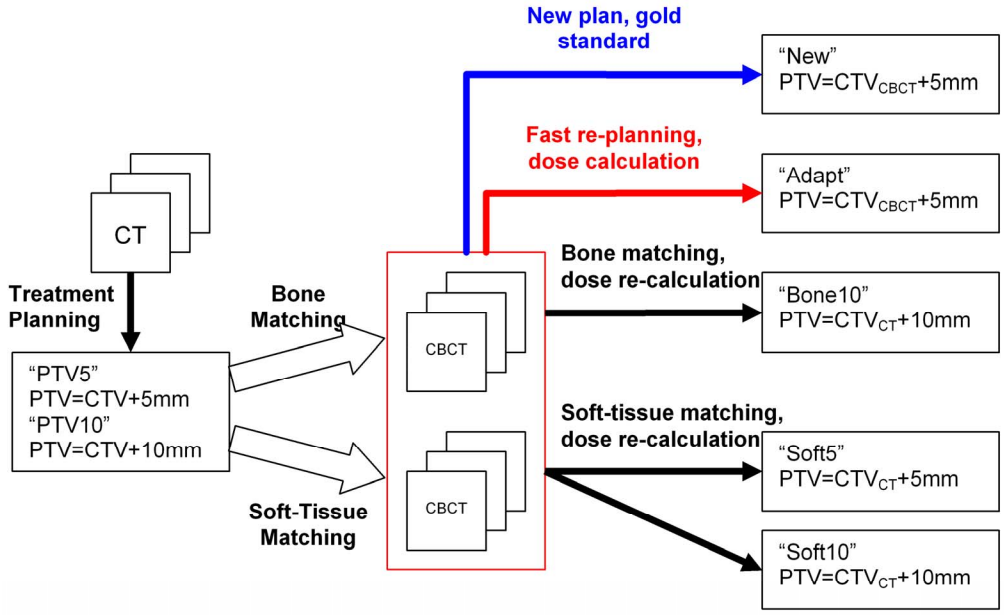

FIG. 1. Online IGRT techniques applied in this clinical study.

Daily CBCT images were acquired using an on-board imaging system (OBI, Varian Medical Systems, Inc., Palo Alto, CA) with the patient in the treatment position prior to any IGRT corrections. The CBCT images were reconstructed with voxel size of 1 mm in-plane and 2.5 mm slice thickness. The daily SOIs were delineated by the same attending physician, so the contouring practice was consistent with original IMRT planning. For each patient, five sets of CBCT images, scanned during the first week of the treatment course, were used in this study. The five fractions provide representative "snapshots" of anatomical variations during the course of treatment, and the delivered dose distribution using each IGRT technique was evaluated on daily basis and as average of the five fractions.

II.B. Online IGRT techniques

Figure 1 illustrates the study design. For each CBCT, three IGRT techniques based on patient repositioning were applied: "bone10", "soft10", and "soft5". Due to couch motion limitations, our current clinical IGRT protocol only performs translational corrections. The matching performed in this study finds the best matching using only these available couch shifts. The bone10 technique relied on finding the translation needed to match the bony structures on the CT with those on the CBCT images. The soft10 and soft5 techniques were performed by finding the translation that yielded the best match between the target contours on CT and the corresponding contours on the CBCT images. The number after each matching technique indicates which IMRT plan was used for that IGRT technique. Thus, the original plans used for bone10, soft10, and soft were "PTV10", "PTV10", and "PTV5", respectively. The PTV5 plan was not used for bone matching as it has already been widely acknowledged that a 5 mm margin is not adequate for this technique. For these patient-repositioning techniques, the dose (from the original treatment plans) was recalculated on the CBCT images with the Eclipse planning system. In addition to the repositioning-based techniques, the online IMRT plan reoptimization technique was also applied to the CBCT images. The 5 mm PTV margin was used for this IGRT technique and the adapted plan is referred as "adapt". The detailed steps of this procedure are explained in the following Sec. II C.

II.C. Online replanning of IMRT plans

Based on our previous work,[28] a linear goal programming model[31] was selected for the online adaptive reoptimization process. The model minimizes the weighted sum of the deviations of the delivered dose from the prescribed (goal) dose. The goal dose was generated by deforming the prescribed dose distribution to match with the daily anatomy on the CBCT. An intensity-based deformable registration algorithm was implemented for this purpose.[32,33] This deformed dose distribution provides the basis for the fast reoptimization algorithm and eliminates the time-consuming trial-and-error process of the DVH-based constraint adjustment. A linear programming (LP) based approach is well suited for online implementation since the solution can be achieved quickly and efficiently using available state-of-the-art LP solvers such as CPLEX (ILOG CPLEX, Sunnyvale, CA). Another advantage of the LP based optimization is that a global solution is always guaranteed once the objective function is properly defined.[34] In our previous optimization model, OAR structures were penalized only for overdoses (e.g., delivered dose exceeds the prescribed dose). In this study, an additional term was introduced in the objective

TABLE I. The mean and standard deviation of minimum CTV dose over five treatment fractions.

	Minimum dose to CTV (Mean ± SD in % prescription dose)						
	Pt. 1	Pt. 2	Pt. 3	Pt. 4	Pt. 5	Pt. #6	No. of Success[a]
Bone10	93.1 ± 12.8	96.7 ± 2.1	65.1 ± 18.8	98.4 ± 0.4	86.5 ± 19.5	95.9 ± 3.5	17
Soft10	98.5 ± 0.9	98.5 ± 0.4	96.4 ± 0.5	98.5 ± 0.4	94.7 ± 10.4	98.9 ± 0.4	22
Soft5	90 ± 11.3	95.3 ± 4.2	90.2 ± 3.3	98.5 ± 1.3	86.5 ± 23.2	98.8 ± 0.7	16
Adapt	99.5 ± 0.8	99.4 ± 0.3	99.3 ± 0.6	99.7 ± 0.4	99.8 ± 0.2	100.2 ± 0.1	30

[a]Number of fractions that minimum dose to CTV >98%.

function to promote further reduction in the dose to the OAR. The reoptimization was, therefore, formulated as follows: Minimize

$$\sum_{i\in T} w_{T,i}(d_i^+ + d_i^-) + \sum_{i\in \mathrm{NT}} w_{\mathrm{NT},i}(d_i^+) + \sum_{i\in \mathrm{OAR}} w_{\mathrm{OAR},i}(d_i^+) - \sum_{i\in \mathrm{OAR}} w_{\mathrm{OAR},i}(d_i^-).$$

Subject to

$$\sum_{j\in B} K_{ij}\omega_j - d_i^+ + d_i^- = D_i^p, \quad i \in T \cup \mathrm{OAR},$$

$$\sum_{j\in B} K_{ij}\omega_j - d_i^+ \le D_i^p, \quad i \in \mathrm{NT},$$

$$0 \le d_i^+ \le UB_O, \quad i \in V,$$

$$0 \le d_i^- \le UB_U, \quad i \in T \cup \mathrm{OAR},$$

$$0 \le \omega_j \le UB_B, \quad j \in B,$$

where T, NT, and OAR represent the structure set containing target voxels, nontarget voxels (e.g., soft-tissue surrounding target and OARs), and OAR voxels, respectively, and total voxels $V=T\cup \mathrm{NT}\cup \mathrm{OAR}$; D_i^p is the prescribed dose at voxel i; w_T, w_{NT}, and w_{OAR} are the priority weights for target, nontarget, and OAR voxel; K_{ij} is the unit dose of beamlet j to voxel i; ω_j is the beamlet intensity of beamlet j; d_i^+/d_i^- are over/underdose at voxel i; UB_O/UB_U are the upper/lower bounds of the dose deviated from the prescription at voxel i; B is the set of active beamlets passing through the SOIs; and UB_B is the bound for the beamlet intensities.

II.D. Dosimetric evaluation

Similar to the previous study,[28] dose distributions were calculated with Eclipse system for plans performed on Eclipse, while dose distributions were calculated with PLUNC for all the adapted plans. The dose calculation was based on intensity maps.

DVHs of the CTV, bladder, and rectum were calculated for the four online IGRT techniques: bone10, soft10, soft5, and adapt. The dosimetric index D_x is defined as the dose to x% of volume of the SOI. The minimum dose to the CTV was defined as $D_{\mathrm{CTV,min}}$ and was derived from the D99. CTV coverage of $D_{\mathrm{CTV,min}}>98\%$ was set as the target coverage criterion. In other words, a given fraction was defined as "successful" if 99% of the CTV volume received at least 98% of the prescription dose. This high coverage limit does not include intrafraction motion. Intrafraction motion on the order of 1–2 mm for prostate treatment has been reported.[35] Such intrafraction motion deteriorates the dose coverage, particularly in the shoulder region of the DVH. Therefore, the tight target coverage of $D_{\mathrm{CTV,min}}>98\%$ criterion was set in this study. Publications on prostate intrafraction motion[36] have indicated that with a seven field plan only 3% of the total fractions were under dosed with a 4 mm margin. Therefore, we anticipate meeting the 95% CTV coverage criteria with 5 mm PTV margin, when intrafraction motion is included.[36]

For each CBCT data set (30 total), the DVHs of the OARs were calculated for each IGRT technique. Three dosimetrical indices, D90, D50, and D30, were compared over the entire data set to evaluate the effectiveness of each technique. The D90, D50, and D30 were chosen as the representatives of the dose sparing in the low, medium, and high dose ranges, respectively. To further assess the OAR sparing provided by online adaptive replanning, a complete new plan ("new" plan) was created (offline) for each CBCT anatomy using the Eclipse planning system. This plan was performed in the same way as the original plan using 5 mm planning margin. The purpose of the new plan is to assess the quality of the adapt plan as the new plan is intended to serve as a gold standard.

In summary, two original IMRT plans with 5 and 10 mm planning margins were performed for each patient. For each of the daily CBCTs, an adapt plan and a new plan were generated, the former one used our new online reoptimization technique, which takes less than 2 min, and the latter one used the commercial planning system, which takes 20–40 min. A total of 30 treatment fractions was studied for all patients, with each fraction having five delivered dose distributions (bone10, soft10, soft5, adapt, and new plans, respectively). The online IGRT techniques, bone10, soft10, soft5, and adapt, were compared for target coverage and OAR sparing at each fraction. OAR sparing was also compared between the adapt and new plans.

III. RESULTS

III.A. Target coverage among IGRT techniques

First, the quality of target coverage during different treatment days was examined. Table I lists the average minimum

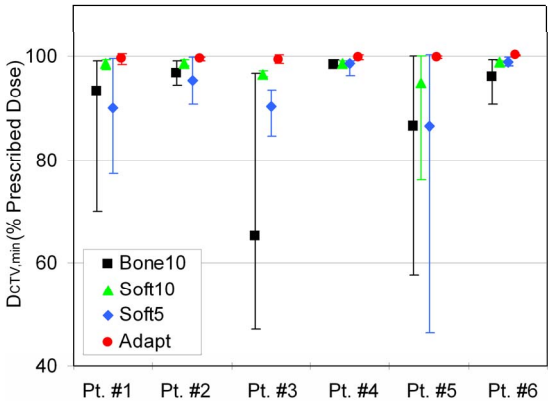

FIG. 2. The $D_{CTV,min}$ (in percentage of prescribed dose) of the six patients delivered by the four IGRT techniques; markers represent the average and error bars represent the range (min/max) over 5 treatment days.

CTV dose ($\bar{D}_{CTV,min}$) and its standard deviation ($SD_{CTV,min}$) over the five treatment fractions for each patient using different IGRT techniques. Figure 2 is the summary illustration of the data. The $\bar{D}_{CTV,min}$ values showed large variations with the bone10 and soft5 techniques, ranging from 65.1% to 98.8% of the prescription dose, while the soft10 and adapt techniques achieved consistent $\bar{D}_{CTV,min}$ coverage at 94.7% or higher of the prescription dose. The standard deviations were also larger with bone10 and soft5 techniques compared with the soft10 and adapt techniques.

The large variations in the mean values and standard deviations indicate that substantial fluctuations in target coverage can occur from day to day with IGRT techniques based on patient repositioning. The last column in Table I lists the number of the successful fractions (i.e., $D_{CTV,min} > 98\%$) achieved using each IGRT technique. Of the total 30 fractions, the bone10, soft10, and soft5 techniques achieved 17, 22, and 16 successful fractions, respectively, while the adapt technique were successful for all 30 fractions. More specifically, the bone10 and the soft5 techniques led to significant daily underdosages for patients 1, 3, and 5. The lowest $D_{CTV,min}$ in 5 days was 70.1%/47.1%/57.6% of the prescribed dose for bone10 technique and was 77.4%/84.6%/46.5% of the prescribed dose for soft5 technique for patients 1, 3, and 5, respectively. The soft10 technique also showed daily underdosage in patient 5 where the lowest minimum target dose in 5 days was 76.2%.

III.B. OAR sparing among IGRT techniques

For each patient, the mean and standard deviation of the daily D90, D50, and D30 were calculated over the five treatment fractions to provide an overall comparison of OAR sparing among the IGRT techniques. Tables II and III summarize these results for the bladder and the rectum, respectively. For the bladder, the adapt technique achieved better overall dose sparing than the other three techniques, with lowest average D90 for all patients and lowest average D50 and D30 for four out of six patients. For the rectum, the adapt technique also showed better sparing than other IGRT techniques, with the lowest average D90 for three out of six patients and lowest average D50 and D30 for five out of six patients.

The bone10 and soft10 techniques resulted in worse OAR sparing compared to the other two techniques partly due to the large planning margins used. For example, the bone10 technique had 17, 13, and 12 fractions with the worst (maximum) D90, D50, and D30 for the bladder, respectively, over the total of 30 fractions. Similarly, it also had 17, 19, and 19 fractions with the worst D90, D50, and D30 for the rectum. The soft10 technique had 17, 17, and 18 worst fractions for the bladder and 11, 10, and 12 worst fractions for the rectums, respectively.

III.C. OAR sparing when target coverage is compromised

Figure 3 shows the daily dosimetric values of the OARs for each IGRT technique and each patient. Interestingly, the

TABLE II. The dose volume indices (D90, D50, and D30) for the bladder.

		Bladder dose volume indices (Mean ± SD in % prescription dose)						No. of best fractions	No. of worst fractions
		Pt. 1	Pt. 2	Pt. 3	Pt. 4	Pt. 5	Pt. 6		
D90	Bone10	23.4 ± 14.7	12.4 ± 12.2	11.3 ± 7.0	30.3 ± 15.2	4.1 ± 2.4	12.0 ± 9.5	2	17
	Soft10	30.5 ± 21.1	13.1 ± 13.7	5.9 ± 3.7	38.0 ± 17.2	4.5 ± 2.6	12.8 ± 8.9	0	17
	Soft5	16.5 ± 14.7	9.9 ± 11.9	3.6 ± 2.4	23.3 ± 11.8	2.9 ± 1.5	10.6 ± 8.7	4	0
	Adapt	9.3 ± 7.7	3.2 ± 4.7	1.8 ± 1.4	19.0 ± 13.4	2.6 ± 1.7	10.0 ± 8.9	24	0
D50	Bone10	74.2 ± 20.9	39.0 ± 20.7	62.6 ± 21.8	79.7 ± 16.7	24.0 ± 7.1	51.6 ± 18.6	2	13
	Soft10	82.8 ± 14.3	42.7 ± 25.4	33.1 ± 12.4	92.5 ± 6.9	28.4 ± 7.4	47.0 ± 15.5	0	17
	Soft5	59.8 ± 23.0	35.3 ± 20.0	22.6 ± 11.1	71.8 ± 12.9	21.3 ± 6.1	40.4 ± 14.9	11	0
	Adapt	44.1 ± 16.5	20.6 ± 15.2	15.6 ± 12.5	71.3 ± 12.9	30.2 ± 6.4	42.0 ± 9.7	17	2
D30	Bone10	91.7 ± 3.5	60.6 ± 25.4	93.6 ± 6.9	97.6 ± 4.8	44.8 ± 12.0	80.6 ± 16.5	5	12
	Soft10	98.2 ± 2.9	64.7 ± 23.1	62.0 ± 13.5	101.0 ± 0.5	55.5 ± 10.1	75.8 ± 13.9	0	18
	Soft5	84.2 ± 12.3	55.5 ± 23.4	47.3 ± 10.9	94.4 ± 4.9	42.0 ± 7.0	66.5 ± 12.0	10	0
	Adapt	69.5 ± 15.2	42.3 ± 17.4	48.9 ± 19.1	92.8 ± 4.9	55.4 ± 7.3	64.3 ± 11.4	15	2

TABLE III. The dose volume indices (D90, D50, and D30) for the rectum.

		Rectum dose volume indices (Mean ± SD in % prescription dose)						No. of best fractions	No. of worst fractions
		Pt. 1	Pt. 2	Pt. 3	Pt. 4	Pt. 5	Pt. 6		
D90	Bone10	68.4 ± 45.2	74.9 ± 41.3	43.6 ± 27.8	56.1 ± 36.7	59.9 ± 46.2	48.4 ± 30.1	2	17
	Soft10	48.9 ± 35.1	67.4 ± 39.2	58.2 ± 32.8	52.5 ± 32.0	40.0 ± 32.5	52.3 ± 30.6	0	11
	Soft5	41.1 ± 30.8	61.9 ± 36.2	45.2 ± 26.2	43.7 ± 25.6	34.1 ± 30.6	48.5 ± 30.1	3	2
	Adapt	32.3 ± 27.6	44.5 ± 32.1	42.6 ± 31.3	51.6 ± 32.3	37.3 ± 31.0	40.3 ± 30.6	25	1
D50	Bone10	61.4 ± 42.9	76.9 ± 30.4	34.7 ± 13.0	66.4 ± 32.0	51.2 ± 42.2	40.7 ± 18.2	6	19
	Soft10	49.0 ± 38.2	65.2 ± 32.9	60.1 ± 27.2	66.1 ± 32.4	41.2 ± 35.3	50.6 ± 25.4	0	10
	Soft5	39.4 ± 34.2	60.1 ± 30.0	47.9 ± 23.9	58.1 ± 29.3	35.1 ± 33.1	43.8 ± 27.8	8	0
	Adapt	35.7 ± 30.5	51.4 ± 25.0	54.6 ± 29.8	56.2 ± 32.3	34.8 ± 31.0	35.3 ± 25.9	16	2
D30	Bone10	77.6 ± 33.9	77.0 ± 28.0	34.1 ± 7.9	83.5 ± 28.8	70.0 ± 35.5	59.9 ± 25.3	6	19
	Soft10	60.5 ± 34.9	71.8 ± 24.5	68.2 ± 21.8	77.3 ± 30.6	54.9 ± 30.6	63.3 ± 23.7	0	12
	Soft5	52.6 ± 31.7	64.6 ± 22.1	54.0 ± 18.0	69.4 ± 29.0	49.1 ± 30.7	61.2 ± 21.1.	5	0
	Adapt	43.2 ± 26.1	56.8 ± 22.3	58.7 ± 24.0	59.4 ± 24.8	47.3 ± 26.9	57.0 ± 22.1	19	1

adapt technique did not achieve the best OAR sparing for all fractions. For the bladder, the adapt technique had 24, 17, and 15 fractions (out of 30 fractions) with best (minimum) D90, D50, and D30 parameters. Moreover for the rectum, the adapt technique had 25, 16, and 19 fractions with best D90, D50, and D30 parameters. When the adapt plans did not score the best for OAR sparing, the apparent gains of the OAR sparing achieved by the other IGRT techniques were accompanied by an underdosage in the target volumes. Case examples are shown below.

Figure 4 shows the DVHs for two patients using each IGRT technique. The gray zone on each DVH plot indicated the range of the daily DVHs over 5 days. The solid black lines on the "CTV-adapt" chart indicated the original planned DVHs for the CTVs. As shown, the adapt technique reproduced the CTV coverage for both patients despite the geometry changes among the CTVs and the OARs. Both bone10 and soft5 techniques resulted in some daily target underdosage for both cases. This indicated repositioning based IGRT techniques may not perform consistently to account for the large target variations.

Due to the missing CTV coverage, the repositioning techniques showed some apparent or false OAR sparing. For the first case [Fig. 4(a)], the bone10 technique showed better bladder DVHs than those of the soft10 and soft5 techniques, as the gray zone for the bone10 was at a lower level compared to either the soft10 or the soft5. For the second case [Fig. 4(b)], the bladder DVHs from any of the repositioning techniques were better than the adapt technique and the bone10 had the best bladder DVHs of all. Therefore, when OAR sparing is compared among IGRT techniques, it is important to distinguish true gains in sparing from false gains due to missing target coverage.

III.D. Adapt plan quality compared with new plan

To further assess the quality of the adapt plans, the dosimetrical metrics of the adapted plans were compared with the "gold standard," i.e., the new plans. The average values of D90, D50, and D30 ($\overline{D90}$, $\overline{D50}$, and $\overline{D30}$, respectively) of the OARs were compared for each patient, as shown in Figs. 5(a) and 5(b).

In the low dose region (represented by $\overline{D90}$), both the adapt and the new plans showed similar OAR sparing for both bladder and rectum. Most discrepancies of the $\overline{D90}$ were within 5% for both the bladder and the rectum, except for the rectum of patient 1, where the adapt plan was about 8% worse than that of the new plan. In the medium and high dose regions (represented by $\overline{D50}$ and $\overline{D30}$), the new plans provided slightly better sparing for both OARs. For the bladder, the new plans had 0%–5% more sparing for five out of six patients, and 5%–10% for one patient. Also for the rectum, the new plans had 0%–5% more sparing for three out of six patients, and 5%–8% for the rest of the patients.

IV. DISCUSSION

This study investigated different online IGRT strategies used to compensate for interfraction uncertainties in prostate IMRT. Techniques based on patient repositioning (bone10, soft10, and soft5) could be sufficient to correct simple geometrical variations where the relative positions of the target volumes and the OARs remain relatively consistent. Figure 6 shows an example of such case. The bone10 and soft10 techniques provided sufficient CTV coverage; however, both techniques spilled high dose into the bladder and rectum due to the large planning margins. For such cases, the performance of the adapt technique is very similar to the soft5 technique, indicating daily imaging and position realignment is adequate.

In this study, complicated positioning changes were observed on the daily CBCT anatomy such as (1) prostate and seminal vesicle locations showed differential positioning changes, and (2) the relative geometry among the OAR and target changed. When the relative position change among SOIs is large, correcting the misalignment between the daily

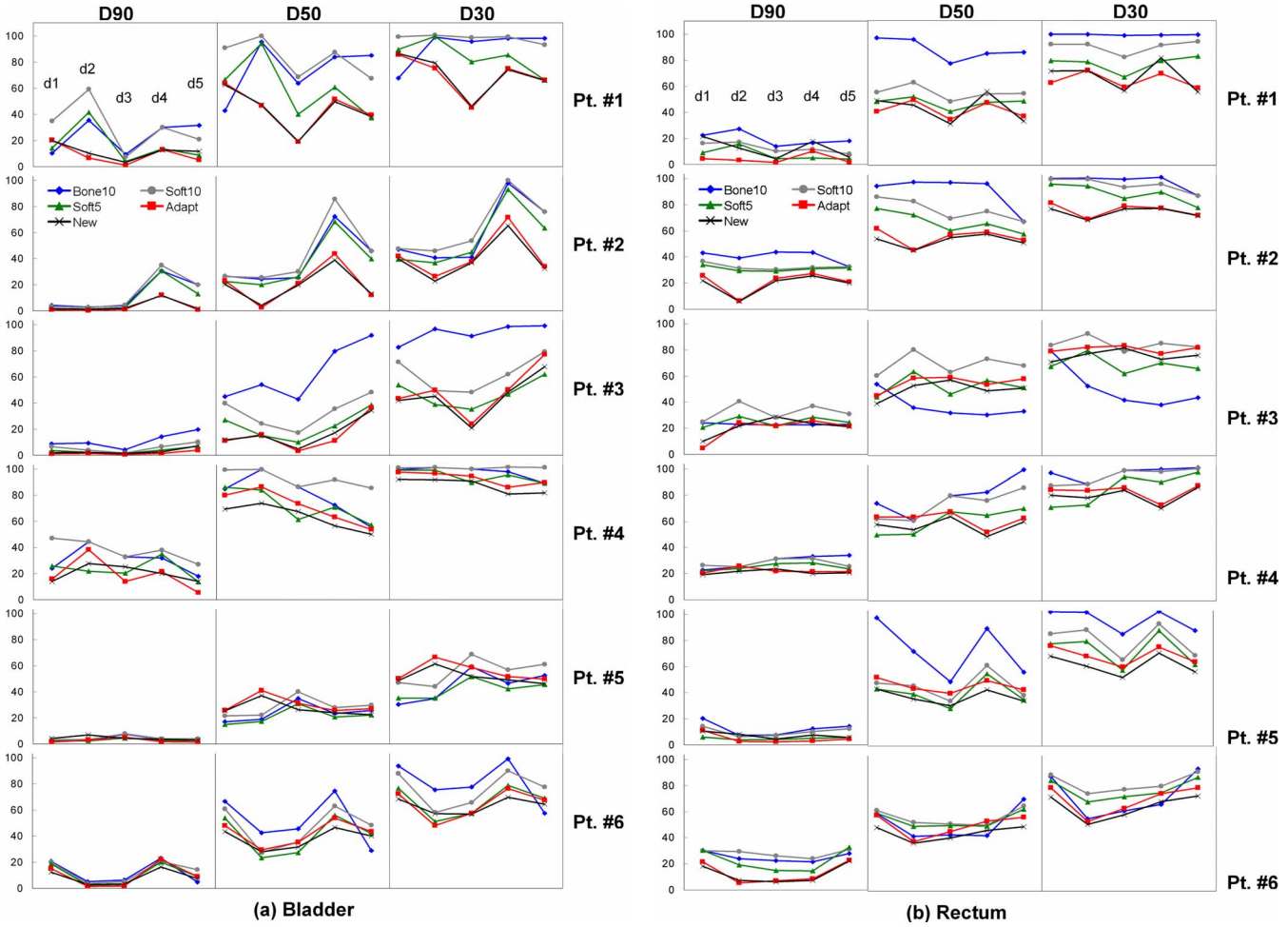

FIG. 3. (a) The daily D90, D50, and D30 of four online correction techniques (bone10, soft10, soft5, and adapt) and the new plan over five treatment days (labeled as d1–d5) for bladder. (b) The daily D90, D50, and D30 of four online correction techniques (bone10, soft10, soft5, and adapt) and the new plan over 5 treatment days (labeled as d1–d5) for rectum.

and planned anatomies using couch shifts alone could lead to regional underdosages to the CTV and some regional overdosages to the OARs. It is acknowledged that the current IGRT protocols only use translational shifts, and if rotational corrections can be made, the results for the positioning based techniques would potentially improve. This would require the upgrade of conventional couches to more advanced ones that allow rotational motions.[20,21] However, the inclusion of rotational corrections would not be able to correct the relative position changes between the prostate and the SV, or the shape/volume changes that occur only to certain segments/parts of the rectum. The prostate and the seminal vesicles commonly present different movements in response to changes in bladder and rectum filling. Also, the OARs may not only vary in volume from day to day but also in shape as well, further complicating the geometrical relationships among OARs and target volumes. An example of such a case is shown in Fig. 7. In this case, the middle part of the rectum showed much larger extension than planned. The missed coverage to the target was worse for the bone10 and soft5 techniques. The bone10 technique could not adjust to the change of the soft-tissue structures relative to the bony anatomy. Due to inadequate margins, the soft5 technique failed to further compensate the relative position variations among SOIs. The soft10 worked the best among the three position correction techniques for this case, yet still lacked the coverage to a small amount of the CTV. All patient position correction techniques showed large portions of high dose deposited to the rectum. The adapt technique consistently covers the entire CTV volume while reducing the dose to the nearby bladder and rectum.

In summary, the effect of IGRT on target coverage and OAR sparing is impacted by two important factors: (1) Planning margin and 2) organ motion. If the plan is performed with 10 mm margin, the OAR sparing would be worse compared with the OAR sparing from a plan using 5 mm margin. With a large margin, the prostate/SV has room to move and still receive adequate dosage. As for the OAR, they already have a relatively large volume receiving a high dose on the prescribed dose distribution, and additional variation will seem less significant in terms of a percentage. When patient anatomy is deformed, the outcomes of the repositioning techniques can show a large variation for plans with a highly conformal dose distribution and small planning margin. In

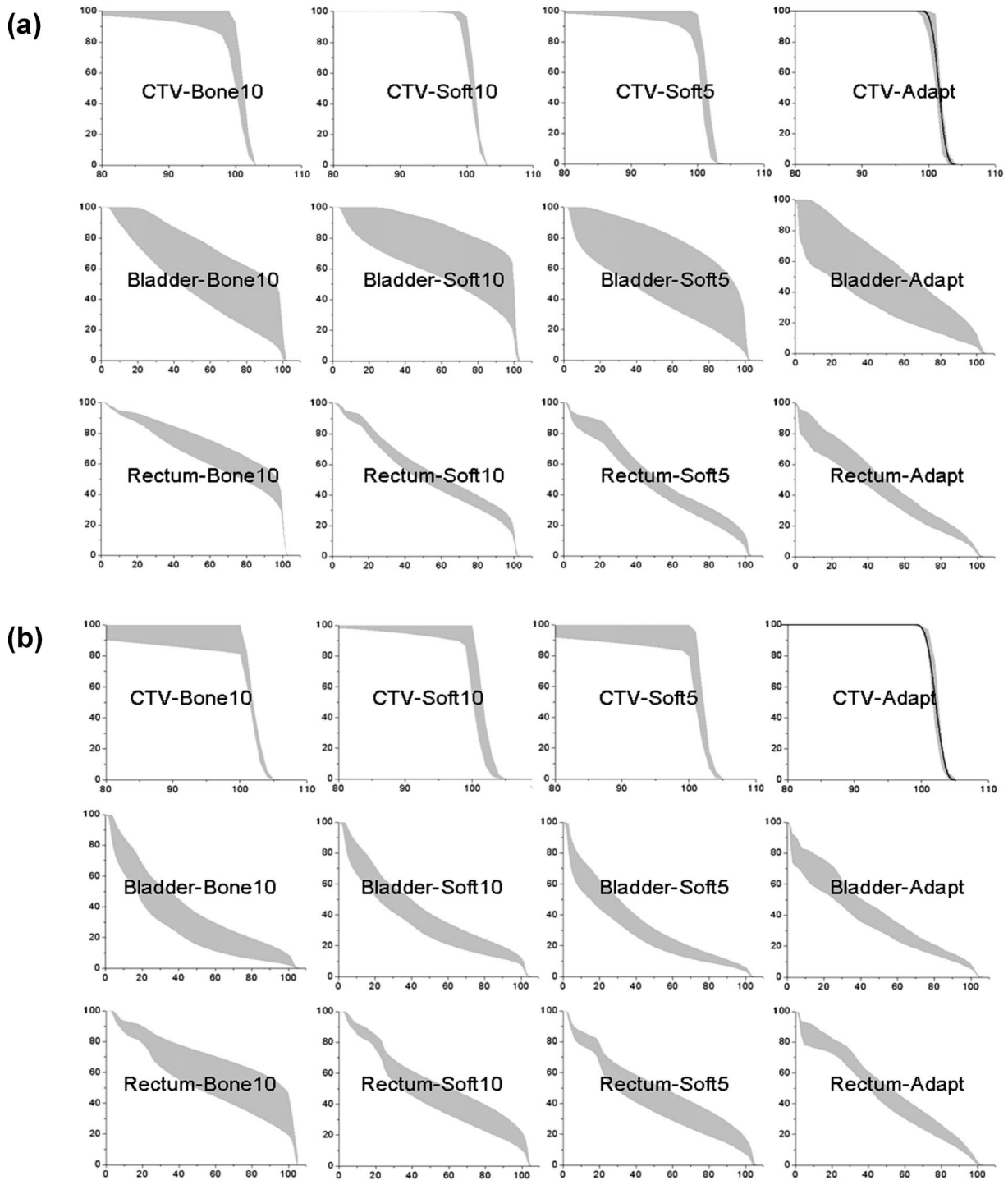

FIG. 4. The CTV and OAR DVH variations of two patients with the four IGRT techniques. The gray zone on each DVH plot indicates the range of the daily DVHs over five days. The solid black lines on the CTV-adapt chart indicate the original planned DVHs for the CTVs.

such cases, the CTV may miss the coverage when any part of the volume is displaced a few mm away from planned position. For cases that target coverage is compromised, it is important to distinguish between the true gains in OAR sparing and false gains due to missing target coverage. For example, if the prescription dose does not fully cover the CTV at the prostate-rectum boundary, then the rectum sparing would potentially get improved. Therefore, for plans with the same planning margin, the gain of OAR sparing from one plan over the other has to be judged in conjunction with CTV coverage.

Results show that the adapt technique allows the use of a smaller PTV margin (e.g., 5 mm in this study) without sacrificing the target coverage. However, this 5 mm PTV margin may not be sufficient for the other repositioning based IGRT techniques when large deformation occur. If a soft-tissue

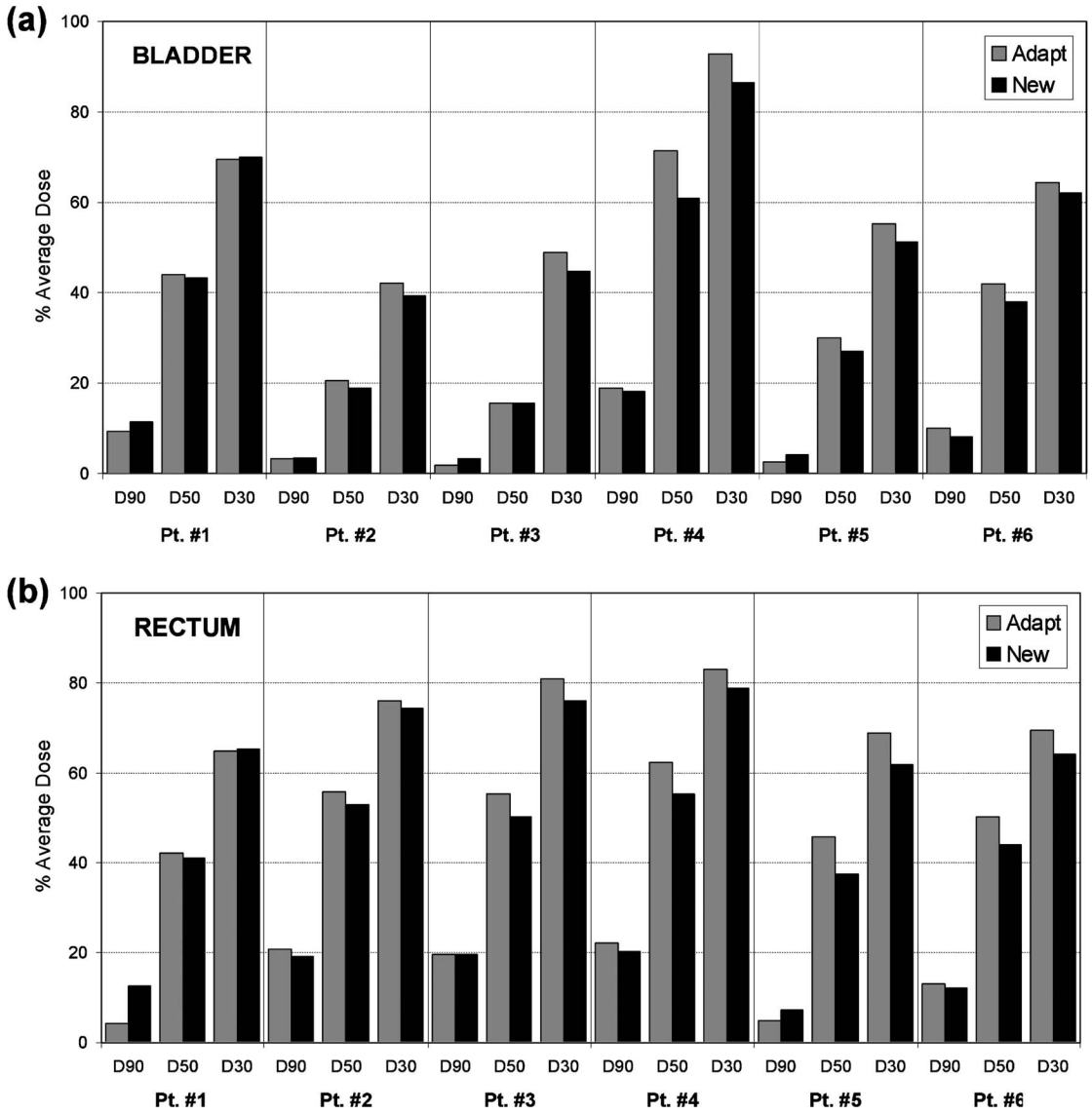

FIG. 5. Dosimetric comparison between plans from the adapt and new plans: (a) D90, D50, and D30 doses to the bladders; and (b) D90, D50, and D30 doses to the rectums. All numbers are the average over 5 treatment days.

matching technique is to be used, a 10 mm PTV margin seems to be adequate for all patients in terms of target coverage. The use of smaller margins (i.e., <5 mm) for the adapt technique may need further clinical study and validation due to the fact that there are other geometric uncertainties,[37–40] such as contouring uncertainties and intrafractional motion.

The observed differences between the position correction techniques and the replanning technique illustrate the fundamental differences in their technical designs. The repositioning techniques only concentrate on the target coverage with no explicit constraint on rectum or bladder sparing for each given CBCT anatomy. The online replanning technique does not suffer from the same limitation, as it reoptimizes the fluence maps by applying dose constraints on both the targets and the OARs. Therefore, the average DVHs of the rectum and bladder among all patients using adapt plans showed better dose sparing to the rectum and bladder compared to those of repositioning techniques. At the current fractionation scheme, the daily DVHs were not the primary concern, as the averaged out or the final cumulative DVHs were of more interest. However, if consistent optimal target coverage and OAR sparing at each single fraction can be achieved without adding extra overall treatment time, it should still be of clinical interest as this field continuous to improve the quality of treatment. For current and future hypofractionated treatment schemes, the online adaptive technique would be of great benefit, as large daily fraction doses delivered over fewer fractions requires daily corrections, rather than averaging over many fractions, to match the original plan.[37–39]

For the conventional IMRT planning, meeting the dose volume based constraints not only depend on the geometry of the PTV and the OARs but also on the volume of the OARs. If the patient had a small bladder, then meeting the bladder constraints would be hard for this patient, while it would be relatively easier to meet the constraints if another

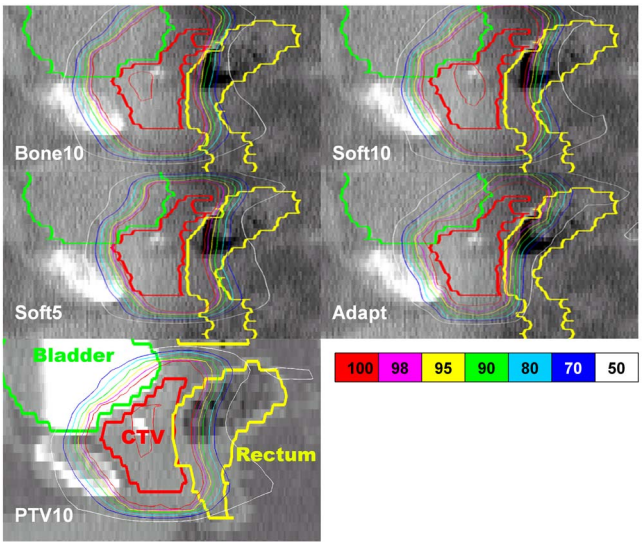

FIG. 6. Dose distributions from one representative day with the four IGRT techniques: bone10, soft10, soft5, adapt, and the original plan, PTV10. The plans from bone10, soft10, soft5, and adapt techniques are overlaid on daily CBCT images while the original plan is overlaid on the planning CT images.

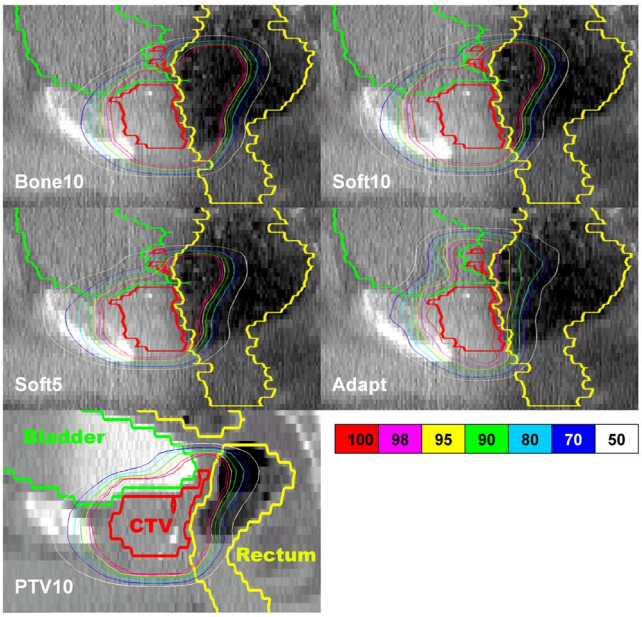

FIG. 7. Dose distributions from one representative day with the four IGRT techniques: bone10, soft10, soft5, adapt, and the original plan, PTV10. The plans from bone10, soft10, soft5, and adapt techniques are overlaid on daily CBCT images while the original plan is overlaid on the planning CT images.

patient had a large bladder. Because of that, these constraints needed to be adjusted during optimization so that we can balance all the constraints and achieve optimal dose distribution for each patient. We refer this as "trial-and-error" adjustment of the dose volume constraints during optimization. Hence, replanning using such conventional IMRT planning algorithms and processes would be time consuming and not suitable for online application.

The primary advantage of the plan adaptation technique over standard IMRT planning techniques is its online implementation with fast planning time. In order to achieve the high speed required for online plan modification, approximations and simplifications have to be made. Some rely on fast manipulation of the aperture shape[24,26,27] or the two-dimensional (2D) intensity map[22] to achieve 3D dose distribution modification. We have proposed a fast reoptimization technique that performs inverse planning using the original plan as a basis.[28] For 30 CBCT fractions, all adapted plans were reoptimized within less than 2 min. The formulation of the optimization problem using goal programming allowed for a consistent speed for all cases. Such high efficiency makes the online adaptive strategy possible for clinical implementation. For future work, we plan to introduce more optimization parameters to allow further flexibility of priority control to differentiate the importance of sparing different OARs and normal tissues. More testing of the robustness of the model with a large pool of patients is also in the plan to establish confidence for clinical implementation.

A current "bottleneck" in online adaptive treatment is the delineation of the daily SOIs, particularly when the image quality of the CBCT is poor. The delineation of daily SOIs not only would take a longer time on images with poor soft-tissue visibility but also may cause larger interobserver variations. The contouring for the CBCT is more challenging even for our attending physician who is specialized in treating prostate cancers. Compared to CT, the CBCT images are noisier and the soft-tissue contrast is also compromised. Therefore, distinguishing the boundaries of the soft-tissue organs (such as prostate, bladder, and rectum) is harder for CBCT. The irregular or nonsmooth boundaries of the contours shown in Figs. 6 and 7 reflect such difficulty. Such limitations are acknowledged but not dealt with in this project, as they are large research areas by themselves. To minimize the impact of these CBCT related limitations, the daily SOIs were defined by the treating physicians in this study. This step may not be the most time efficient; however, we felt it is the most accurate one given the current CBCT configuration. Another way to alleviate the time consuming contouring process is to directly transfer contours from CT to CBCT using the deformation field already created by the deformable registration.[40] We expect that the CBCT image quality will continue to improve with hardware and reconstruction software advances by vendors and with robust techniques for autocontouring and contour-propagation techniques developed by users. All together, we anticipate this bottleneck will be removed in the near future so that online adaptive treatment can be realized in the clinic.

The nosier boundary from CBCT structures would affect the quality of the deformable registration. Moreover the inaccuracy of the registration will be carried into the dose distribution. In this study, we took several steps to minimize the effect of this problem. First, the contours were smoothed prior to deformable registration to ensure the mapping of the organ was relatively smooth in all directions. Second, the deformable registration algorithm itself had a smoothness term, which ensured that each voxel's displacement was relatively coherent with its neighboring voxels. For the final

dose calculation and DVH comparison, we still used the original contours (unsmoothed). The irregular boundary would have less effect on the reoptimization compared to other processes in this study. The 5 mm expansion from CTV to PTV would make the PTV boundaries smooth. This is evident in Figs. 6 and 7 as the isodose lines are quite smooth.

In this study, the daily dose distributions were calculated using the CBCT images. The inconsistency of the Hounsfield unit (HU) values will affect the accuracy of the dose calculation for plans based on CBCT. Our own experiment on the current CBCT configuration showed that this effect was less than 1%.[41,42] The maximum HU difference between CBCT and CT of the Catphan phantom was 34 HU in the Teflon. The differences in other materials were less than 10 HU. The scatter and artifacts in CBCT became severe in the surrounding inhomogeneous tissues with reduced HU values up to 200 HU. However, the MU/cGy differences were less than 1% for most phantom cases. This also should improve as CBCT techniques improve.

V. CONCLUSIONS

The new IGRT technique using online plan adaptation (reoptimization) was compared to techniques based on patient repositioning for six prostate IMRT patients using 30 treatment fractions with CBCT. Results demonstrated that it is feasible to reoptimize the treatment plan online. All IGRT techniques can be sufficient to correct simple geometrical variations where the relative positions of the target volumes and the OARs remain relatively consistent. However, the adapted plans showed significant benefits when a high degree of deformation or differential organ position displacement occurred. For these cases, the online reoptimization technique can be a highly valuable IGRT tool to compensate for daily treatment uncertainties, especially when a hypofractionated scheme is applied and daily correction, rather than averaging over many fractions, is required to match the original plan.

ACKNOWLEDGMENT

The authors would like to thank Dr. Boonyanit Mathayomchan for his contribution to this study. This study is partially funded by a research grant from Varian Medical Systems.

[a]Author to whom correspondence should be addressed. Electronic mail: jackie.wu@duke.edu; Telephone: (919)681-1841; Fax: (919)681-7183.

[1]"ICRU Report 50 International Commision on Radiation Units and Measurements," ICRU Report No. 50, 1993.
[2]"ICRU Report 62 International Commision on Radiation Units and Measurements," ICRU Report No. 62, 1999.
[3]M. van Herk, "Errors and margins in radiotherapy," Semin. Radiat. Oncol. **14**, 52–64 (2004).
[4]M. van Herk, P. Remeijer, and J. Lebesque, "Inclusion of geometric uncertainties in treatment plan evaluation," Int. J. Radiat. Oncol., Biol., Phys. **52**, 1407–1422 (2002).
[5]J. C. Stroom and P. R. M. Storchi, "Automatic calculation of three-dimensional margins around treatment volumes in radiotherapy planning," Phys. Med. Biol. **42**, 745–755 (1997).
[6]J. Bijhold, M. van Herk, R. Vijlbrief, and J. V. Lebesque, "Fast evaluation of patient set-up during radiotherapy by aligning features in portal and simulator images," Phys. Med. Biol. **36**, 1665–1679 (1991).
[7]K. G. A. Gilhuijs and M. van Herk, "Automatic on-line inspection of patient setup in radiation therapy using digital portal images," Med. Phys. **20**, 667–677 (1993).
[8]G. Remeijer, G. Ploeger, M. van Herk, and J. Lebesque, "3-D portal image analysis in clinical practice: An evaluation of 2-D and 3-D analysis techniques as applied to 30 prostate cancer patients," Int. J. Radiat. Oncol., Biol., Phys. **46**, 1281–1290 (2000).
[9]M. Jobse, J. Davelaar, E. Hendriks, R. Kattevilder, H. Reiber, and B. Stoel, "A new algorithm for the registration of portal images to planning images in the verification of radiotherapy, as validated in prostate treatments," Med. Phys. **30**, 2274–2281 (2003).
[10]H. S. Jans, A. M. Syme, S. Rathee, and B. G. Fallone, "3D interfractional patient position verification using 2D-3D registration of orthogonal images," Med. Phys. **33**, 1420–1439 (2006).
[11]K. G. A. Gilhuijs, P. J. H. van de Ven, and M. van Herk, "Automatic three-dimensional inspection of patient setup in radiation therapy using portal images, simulator images, and computed tomography data," Med. Phys. **23**, 389–399 (1996).
[12]S. Jaffray, J. Siewerdsen, J. Wong, and A. Martinez, "Flat-panel cone-beam computed tomography for image-guided radiation therapy," Int. J. Radiat. Oncol., Biol., Phys. **53**, 1337–1349 (2002).
[13]E. Rijkhorst, M. van Herk, J. Lebesque, and J. Sonke, "Strategy for online correction of rotational organ motion for intensity-modulated radiotherapy of prostate cancer," Int. J. Radiat. Oncol., Biol., Phys. **69**, 1608–1617 (2007).
[14]A. D. Lauve, J. V. Siebers, A. J. Crimaldi, M. P. Hagan, and P. J. Keall, "A dynamic compensation strategy to correct patient-positioning errors in conformal prostate radiotherapy," Med. Phys. **33**, 1879–1887 (2006).
[15]L. Court, L. Dong, A. Lee, M. Bonnen, J. O'Daniel, H. Wang, R. Mohan, and D. Kuban, "An automatic CT-guided adaptive radiation therapy technique by online modification of multileaf collimator leaf positions for prostate cancer," Int. J. Radiat. Oncol., Biol., Phys. **62**, 154–163 (2005).
[16]G. H. Olivera, E. E. Fitchard, P. J. Reckwerdt, K. J. Ruchala, and T. Mackie, "Delivery modification as an alternative to patient repositioning in tomotherapy, in *The Use of Computers in Radiation Therapy*, edited by W. Schlegel and T. Bortfeld (Springer, Heidelberg, 2000), pp. 297–299.
[17]Q. Wu, G. Ivaldi, J. Liang, D. Lockman, D. Yan, and A. Martinez, "Geometric and dosimetric evaluations of an online image-guidance strategy for 3D-CRT of prostate cancer," Int. J. Radiat. Oncol., Biol., Phys. **64**, 1596–1609 (2006).
[18]L. E. Court, R. B. Tishler, J. Petit, R. Cormack, and L. Chin, "Automatic online adaptive radiation therapy techniques for targets with significant shape change: A feasibility study," Phys. Med. Biol. **51**, 2493–2501 (2006).
[19]Y. Feng, C. Castro-Pareja, R. Shekhar, and C. Yu, "Direct aperture deformation: an interfraction image guidance strategy," Med. Phys. **33**, 4490–4498 (2006).
[20]N. Linthout, D. Verellen, K. Tournel, T. Reynders, M. Duchateau, and G. Storme, "Assessment of secondary patient motion induced by automated couch movement during on-line 6 dimensional repositioning in prostate cancer treatment," Radiother. Oncol. **83**, 168–174 (2007).
[21]M. Guckenberger, J. Meyer, J. Wilbert, K. Baier, O. Sauer, and M. Flentje, "Precision of image-guided radiotherapy (IGRT) in six degrees of freedom and limitations in clinical practice," Strahlenther. Onkol. **183**, 307–313 (2007).
[22]R. Mohan, X. Zhang, H. Wang, Y. Kang, X. Wang, H. Liu, K. Ang, D. Kuban, and L. Dong, "Use of deformed intensity distributions for on-line modification of image-guided IMRT to account for interfractional anatomic changes," Int. J. Radiat. Oncol., Biol., Phys. **61**, 1258–1266 (2005).
[23]W. Song, B. Bauman, and V. Dyk, "Dosimetric evaluation of daily rigid and nonrigid geometric correction strategies during on-line image-guided radiation therapy (IGRT) of prostate cancer," Med. Phys. **34**, 352–365 (2007).
[24]D. Yan, D. Lockman, D. Brabbins, L. Tyburski, and A. Martinez, "An off-line strategy for constructing a patient-specific planning target volume in adaptive treatment process for prostate cancer," Int. J. Radiat. Oncol., Biol., Phys. **48**, 289–302 (2000).
[25]P. Nijkamp, "Adaptive radiotherapy for prostate cancer using kilovoltage cone-beam computed tomography: First clinical results," Int. J. Radiat. Oncol. Biol. Phys. **70**, 75–82 (2008).
[26]T. Nuver, M. Hoogeman, P. Remeijer, M. van Herk, and J. Lebesque, "An adaptive off-line procedure for radiotherapy of prostate cancer," Int. J. Radiat. Oncol., Biol., Phys. **67**, 1559–1567 (2007).

[27]D. Yan, F. Vicini, J. Wong, and A. Martinez, "Adaptive radiation therapy," Phys. Med. Biol. **42**, 123–132 (1997).
[28]Q. J. Wu, D. Thongphiew, Z. Wang, B. Mathayomchan, V. Chankong, W. R. Lee, and F. F. Yin, "On-line re-optimization of prostate IMRT plans for adaptive radiation therapy," Phys. Med. Biol. **53**, 673–691 (2008).
[29]P. Kupelian, K. Langen, O. Zeidan, S. Meeks, W. Willoughby, T. Wagner, S. Jeswani, K. Ruchala, J. Haimerl, and G. Jeswani, "Daily variations in delivered doses in patients treated with radiotherapy for localized prostate cancer," Int. J. Radiat. Oncol., Biol., Phys. **66**, 876–882 (2006).
[30]Eclipse Algorithm Reference Guide, V. M. Systems, Palo Alto, CA, 2006.
[31]M. D. M. Chankong, *Theory and Methodology* (Dover, New York, 2008).
[32]W. Lu, M.-L. Chen, G. H. Olivera, K. J. Ruchala, and T. R. Mackie, "Fast free-form deformable registration via calculus of variations," Phys. Med. Biol. **49**, 3067–3087 (2004).
[33]G. E. Christensen, R. D. Rabitt, and M. I. Miller, "Deformable templates using large deformation kinematics," IEEE Trans. Med. Imaging **5**, 1435–1447 (1996).
[34]L. S. Lasdon, *Optimization Theory for Large Systems* (Dover, New York, 2002).
[35]B. Madsen, R. Hsi, H. Pham, J. Presser, L. Esagui, L. Myers, and D. Jones, "Intrafractional stability of the prostate using a stereotactic radiotherapy technique," Int. J. Radiat. Oncol., Biol., Phys. **57**, 1285–1291 (2003).
[36]B. Pierburg, P. Parikh, M. Roy, P. Kupelian, A. Mahadevan, G. Weinstein, C. Enke, N. Flores, D. Beyer, and L. Levine, "Dosimetric consequences of intrafraction prostate motion on patients enrolled on multi-institutional hypofractionation study," Int. J. Radiat. Oncol., Biol., Phys. **69**, S23–S24 (2007).
[37]B. Schaly, G. S. Bauman, J. J. Battista, and J. Van Dyk, "Validation of contour-driven thin-plate splines for tracking fraction-to-fraction changes in anatomy and radiation therapy dose mapping," Phys. Med. Biol. **50**, 459–475 (2005).
[38]M. Ghilezan, D. Jaffray, J. Siewerdsen, M. van Herk, A. Shetty, M. Sharpe, Z. Jafri, F. Vicini, R. Matter, and D. Brabbins, "Prostate gland motion assessed with cine-magnetic resonance imaging (cine-MRI)," Int. J. Radiat. Oncol., Biol., Phys. **62**, 406–417 (2005).
[39]D. Létourneau, A. Martinez, D. Lockman, D. Yan, C. Vargas, G. Ivaldi, and J. Wong, "Assessment of residual error for online cone-beam CT-guided treatment of prostate cancer patients," Int. J. Radiat. Oncol., Biol., Phys. **62**, 1239–1246 (2005).
[40]M. Chao, T. Li, E. Schreibmann, A. Koong, and L. Xing, "Automated contour mapping with a regional deformable model," Int. J. Radiat. Oncol., Biol., Phys. **70**, 599–608 (2008).
[41]S. Yoo, G.-T. Kim, R. Hammoud, E. Elder, T. Pawlicki, H. Guan, T. Fox, G. Luxton, and F.-F. Yin, "A quality assurance program for the on-board imagers," Med. Phys. **33**, 4431–4447 (2006).
[42]S. Yoo and F. Yin, "Dosimetric feasibility of cone-beam CT-based treatment planning compared to CT-based treatment planning," Int. J. Radiat. Oncol., Biol., Phys. **66**, 1553–1561 (2006).